# Supporting Information

## Besson and Dumais 10.1073/pnas.1011866108

Besson and Dumais

### SI Text

**The Geometry of Errera's Rule.** In this section, we show that the shortest wall dividing a cell into daughter cells of equal size must be an arc of circle meeting the cell surface at right angle. In order to provide the reader with a geometric interpretation of this result, we first describe the division of a polygonal cell by $N$ connected line segments. We then show that in the limit where $N \to \infty$ these straight segments converge to an arc of circle. We finally extend this result to an arbitrary cell geometry using the calculus of variations.

***Division of a cell by a straight line*** *$(N = 1)$.* Let us consider a polygonal cell divided into two equal parts by a straight line. The dividing line meets two cell edges at distances $l_1$ and $l_2$ from their point of intersection $O$ (Fig. S1*A*). The length of the line $L_1$ and the enclosed area $A_1$ can be expressed as functions of $l_1$, $l_2$ and the angle between the edges $\theta$:

$$L_1 = (l_1^2 + l_2^2 - 2l_1 l_2 \cos\theta)^{\frac{1}{2}}, \quad \textbf{[S1]}$$

$$A_1 = \frac{1}{2} l_1 l_2 \sin\theta. \quad \textbf{[S2]}$$

(Note: although the area $A_1$ includes a small region outside the cell, the derivation to follow is not affected because the outside region has fixed area irrespective of the value of $l_1$ and $l_2$.) We want to find the straight line of shortest length dividing this sector into a closed surface of area $A_0$. Formally, this requires the minimization of the functional $I_1(l_1,l_2,\theta) = L_1(l_1,l_2,\theta) - \lambda A_1(l_1,l_2,\theta)$, where $\lambda$ is the Lagrange multiplier; that is,

$$dI_1 = dl_1\left(\frac{l_1 - l_2\cos\theta}{L_1} - \frac{\lambda}{2} l_2 \sin\theta\right) + dl_2\left(\frac{l_2 - l_1\cos\theta}{L_1} - \frac{\lambda}{2} l_1 \sin\theta\right) = 0. \quad \textbf{[S3]}$$

Because Eq. **S3** must be true independently of the values of $dl_1$ and $dl_2$, we must satisfy the system of equations:

$$\frac{l_1 - l_2\cos\theta}{L_1} - \frac{\lambda}{2} l_2 \sin\theta = 0, \quad \textbf{[S4]}$$

$$\frac{l_2 - l_1\cos\theta}{L_1} - \frac{\lambda}{2} l_1 \sin\theta = 0. \quad \textbf{[S5]}$$

Solving the system **S4**, **S5** gives $l_1 = l_2$ and the value of $l_1$ is determined by the relation $A_1 = A_0$. This result has a simple geometrical interpretation: The median of the shortest dividing line is coincident with the bisector of the angle $\theta$.

***Division of a sector by two line segments*** *$(N = 2)$.* In this second case, the same cell is divided by two connected line segments (Fig. S1*B*). The first segment (respectively, second) meets the edge at distance $l_1$ (respectively, $l_3$) from $O$ and defines a triangle with an opposite angle $\theta_1$ (respectively, $\theta - \theta_1$). The two segments meet at distance $l_2$ from $O$. As above, we can express the length of the segmented line $L_2$ and area of the enclosed region $A_2$ as a function of $l_1$, $l_2$, $l_3$, $\theta$, and $\theta_1$:

$$L_2 = (l_1^2 + l_2^2 - 2l_1 l_2 \cos\theta_1)^{\frac{1}{2}} + (l_2^2 + l_3^2 - 2l_2 l_3 \cos(\theta - \theta_1))^{\frac{1}{2}}, \quad \textbf{[S6]}$$

$$A_2 = \frac{1}{2} l_1 l_2 \sin\theta_1 + \frac{1}{2} l_2 l_3 \sin(\theta - \theta_1). \quad \textbf{[S7]}$$

Once again, minimizing the functional $I_2 = L_2 - \lambda A_2$ leads to a system of equations:

$$\frac{l_1 - l_2\cos\theta_1}{L_{2a}} - \frac{\lambda}{2} l_2 \sin\theta_1 = 0, \quad \textbf{[S8]}$$

$$\frac{l_3 - l_2\cos(\theta - \theta_1)}{L_{2b}} - \frac{\lambda}{2} l_1 \sin(\theta - \theta_1) = 0, \quad \textbf{[S9]}$$

$$\frac{l_2 - l_1\cos\theta_1}{L_{2a}} + \frac{l_2 - l_3\cos(\theta - \theta_1)}{L_{2b}} - \frac{\lambda}{2} l_1 \sin\theta_1 - \frac{\lambda}{2} l_3 \sin(\theta - \theta_1) = 0, \quad \textbf{[S10]}$$

$$\frac{l_1 l_2 \sin(\theta - \theta_1)}{L_{2a}} + \frac{l_2 l_3 \sin(\theta - \theta_1)}{L_{2b}} - \frac{\lambda}{2} l_1 l_2 \cos\theta_1 + \frac{\lambda}{2} l_1 l_3 \cos(\theta - \theta_1) = 0. \quad \textbf{[S11]}$$

The system of Eqs. **S8–S11** is satisfied for

$$\theta_1 = \theta - \theta_1 = \frac{\theta}{2}, \quad \textbf{[S12]}$$

$$l_1 = l_2 = l_3. \quad \textbf{[S13]}$$

Geometrically, each individual segment behaves as if dividing half of the polygonal cell with shortest length and with its median going through $O$ as for $N = 1$.

***Division of a sector by $N$ line segments.*** The problem presented in the last sections can further be extended to the division of a sector by $N$ connected segments (Fig. S1*C*). The final result can be inferred from the results for $N = 1$ and $N = 2$. By induction, each segment will subdivide into two segments of equal lengths with their medians meeting at $O$.

Formally, we consider $N$ segments defining $N$ triangles of angles $\theta_i$ and side lengths $l_i$ and $l_{i+1}$. The first and last segments meet the cell edges at distances $l_1$ and $l_{N+1}$ from $O$, respectively, and the angles $\theta_i$ must satisfy the constraint $\sum_i \theta_i = \theta$. The total length of the segmented line $L_N$ and enclosed area $A_N$ are

$$L_N = \sum_{i=1}^{N} (l_i^2 + l_{i+1}^2 - 2l_i l_{i+1} \cos\theta_i)^{\frac{1}{2}}, \quad \textbf{[S14]}$$

$$A_N = \sum_{i=1}^{N} \frac{1}{2} l_i l_{i+1} \sin\theta_i. \quad \textbf{[S15]}$$

Using the same variational approach, the minimization of $I_N = L_N - \lambda A_N$ leads to the generic relationships

$$\theta_1 = \ldots = \theta_N = \frac{\theta}{N}, \quad \textbf{[S16]}$$

$$l_1 = \ldots = l_{N+1}. \quad \textbf{[S17]}$$

The expression of the total length $L_N$ as a function of $N$, $\theta$, and $A_0$ can be derived by substituting Eqs. **S16** and **S17** in Eqs. **S14** and **S15** with the constraint $A_N = A_0$.

$$L_N = 2\left(\frac{NA_0}{\sin(\frac{\theta}{N})}\left(1 - \cos\left(\frac{\theta}{N}\right)\right)\right)^{\frac{1}{2}}. \quad \textbf{[S18]}$$

***Continuous limit*** *($N \to \infty$)*. In the continuous limit, each point on the dividing curve has its tangent normal to the line joining it to the sector's center. This geometrically defines an arc of circle centered at $O$. The length of this curved wall $L_c$ corresponds to the limit of Eq. **S18** when $N \to \infty$.

$$L_c = \lim_{N\to\infty} L_N = 2\left(\frac{A_0\theta}{2}\right)^{\frac{1}{2}}. \quad \textbf{[S19]}$$

Because we want to compare the length of the straight and the curved line independently of the area $A_0$, we will consider the ratio between $L_c$ and $L_s = L_1$.

$$r = \frac{L_c}{L_s} = \left(\frac{\theta \sin\theta}{2(1 - \cos\theta)}\right)^{\frac{1}{2}}. \quad \textbf{[S20]}$$

The function $r(\theta)$ is always smaller or equal to 1 (Fig. S1*D*) proving that the curved wall enclosing a surface of fixed area $A_0$ is always shorter than the straight line under the same conditions.

***Formal approach using the calculus of variations.*** In the general case, the cellular boundary can be described by a function $f(x)$ (Fig. S1*E*). We attempt to construct a curve of equation $y(x)$ of minimal length enclosing a surface of area $A_0$. This curve is bound by two points of coordinates $(x_1 f(x_1))$ and $(x_2 f(x_2))$. The length of the dividing wall $L$ and the subsequent area of the daughter cell $A$ can be written as a function of $y$, $f$, $x_1$, and $x_2$.

$$L = \int_{x_1}^{x_2} (1 + y'(x)^2)^{\frac{1}{2}} dx, \quad \textbf{[S21]}$$

$$A = \int_{x_1}^{x_2} y(x)dx - \int_{x_1}^{x_2} f(x)dx. \quad \textbf{[S22]}$$

We want to find the form of the function $y$ that minimizes the function $I = L + \lambda A$, where $\lambda$ is the Lagrange multiplier. We introduce the functional $\Phi(x,y,y')$ as

$$I = \int_{x_1}^{x_2} ((1 + y'(x)^2)^{\frac{1}{2}} + \lambda y(x) - \lambda f(x))dx, \quad \textbf{[S23]}$$

$$= \int_{x_1}^{x_2} (\Phi(x,y,y') - \lambda f(x))dx. \quad \textbf{[S24]}$$

Considering the family of curves $Y = y + \alpha\delta y$, we have $Y' = y' + \alpha\delta y', X_1 = x_1 + \alpha\delta x_1, X_2 = x_2 + \alpha\delta x_2$ and the functional $I(\alpha)$ writes as

$$I(\alpha) = \int_{X_1}^{X_2} (\Phi(x,Y,Y') - \lambda f(x))dx. \quad \textbf{[S25]}$$

A necessary condition for $I(\alpha)$ to be a minimum when $\alpha = 0$ is that $I'(\alpha) = \frac{dI}{d\alpha}$ must be zero when $\alpha = 0$.

$$I'(\alpha) = \int_{X_1}^{X_2} \left(\frac{\partial\Phi}{\partial Y}\delta y + \frac{\partial\Phi}{\partial Y'}\delta y'\right)dx + [\Phi(x,Y,Y') - \lambda f]_{X_2}\delta x_2 - [\Phi(x,Y,Y') - \lambda f]_{X_1}\delta x_1. \quad \textbf{[S26]}$$

When $\alpha = 0$, the integral derivative writes as

$$I'(0) = \int_{x_1}^{x_2} \left(\frac{\partial\Phi}{\partial y}\delta y + \frac{\partial\Phi}{\partial y'}\delta y'\right)dx + [\Phi(x,y,y') - \lambda f]_{x_2}\delta x_2 - [\Phi(x,y,y') - \lambda f]_{x_1}\delta x_1. \quad \textbf{[S27]}$$

Integrating by parts, the first term of Eq. **S27** becomes

$$I'(0) = \int_{x_1}^{x_2} \left(\frac{\partial\Phi}{\partial y} - \frac{d}{dx}\frac{\partial\Phi}{\partial y'}\right)\delta y dx + \left[\frac{\partial\Phi}{\partial y'}\delta y\right]_{x_2} - \left[\frac{\partial\Phi}{\partial y'}\delta y\right]_{x_1} + [\Phi - \lambda f]_{x_2}\delta x_2 - [\Phi - \lambda f]_{x_1}\delta x_1. \quad \textbf{[S28]}$$

Using the expression of the boundary conditions $(\delta y)_i = (f' - y')\delta x_i + \epsilon_i$, we have

$$I'(0) = \int_{x_1}^{x_2} \left(\frac{\partial\Phi}{\partial y} - \frac{d}{dx}\frac{\partial\Phi}{\partial y'}\right)\delta y dx + \left[\frac{\partial\Phi}{\partial y'}\left(f' - y' + \frac{\epsilon_2}{\delta x_2}\right) + \Phi - \lambda f\right]_{x_2}\delta x_2 - \left[\frac{\partial\Phi}{\partial y'}\left(f' - y' + \frac{\epsilon_1}{\delta x_1}\right) + \Phi - \lambda f\right]_{x_1}\delta x_1. \quad \textbf{[S29]}$$

To have the minimum condition $I'(0) = 0$ independently of the values of $\delta x_1$ and $\delta x_2$, we must meet a system of three equations **S30–S32**. The first equation is known as the Euler–Lagrange equation and the two next ones are boundary conditions.

$$\frac{\partial\Phi}{\partial y} - \frac{d}{dx}\frac{\partial\Phi}{\partial y'} = 0, \quad \textbf{[S30]}$$

$$\left[\frac{\partial\Phi}{\partial y'}(f' - y') + \Phi - \lambda f\right]_{x_1} = 0, \quad \textbf{[S31]}$$

$$\left[\frac{\partial\Phi}{\partial y'}(f' - y') + \Phi - \lambda f\right]_{x_2} = 0. \quad \textbf{[S32]}$$

After substitution of $\Phi$ by its expression, the system becomes

$$\frac{d}{dx}\frac{y'}{(1 + y'^2)^{\frac{1}{2}}} = -\lambda, \quad \textbf{[S33]}$$

$$\left[\frac{1 + y'f'}{(1 + y'^2)^{\frac{1}{2}}} + \lambda(y - f)\right]_{x_1} = 0, \quad \textbf{[S34]}$$

$$\left[\frac{1+y'f'}{(1+y'^2)^{\frac{1}{2}}}+\lambda(y-f)\right]_{x_2}=0. \quad \textbf{[S35]}$$

The Euler–Lagrange equation can be integrated twice and the boundary conditions can be simplified by using the relationships $y(x_1)=f(x_1)$ and $y(x_2)=f(x_2)$. The minimization of $I$ gives two identities defining an arc of circle meeting orthogonally the boundary of the mother cell.

$$(x-x_0)^2+(y-y_0)^2=\frac{1}{\lambda^2}, \quad \textbf{[S36]}$$

$$[y'f']_{x_1}=[y'f']_{x_2}=-1. \quad \textbf{[S37]}$$

Note that this result can be extended to three dimensions when considering the division of a body of volume $V$ by a surface of area $S$ enclosing a fixed volume $V_0$. Minimization of the function $I=S+\lambda V$ using the calculus of the variations yields the division plane should be a surface of constant mean curvature meeting orthogonally the body's boundary.

**Derivation of Maximum Entropy Model.** In this section, we derive the equations for the distribution of endoplasmic microtubules populating the cytoplasmic strands of a two-dimensional polygonal cell with $m$ sides.

We recall $x^u$ is the density of microtubules connecting the nucleus to edge $u$. We posit that the microtubules adopt the distribution with the highest number of configurations. For the discrete distribution $(x^1..x^m)$, the number of configurations is measured by the Shannon entropy, $H$:

$$H(x^1..x^m)=-\sum_{u=1}^{m}x^u\ln(x^u). \quad \textbf{[S38]}$$

We use the method of the Lagrange multipliers to find the distribution maximizing the function $H(x^1..x^m)$ subject to all the constraints on the system. Each constraint is given by a function $g_i(x^1..x^m)$, and we are interested in points where $g_i(x^1..x^m)=0$. The first constraint arises from the fact that the relative densities $x^u$ must account for all microtubules:

$$g_1(x^1..x^m)=1-\sum_{u=1}^{m}x^u. \quad \textbf{[S39]}$$

To account for this first constraint, we construct the Lagrangian $L_1(x^1..x^m,\alpha)$ as

$$L_1(x^1..x^m,\alpha)=-\sum_{u=1}^{m}x^u\ln(x^u)+\alpha\left(1-\sum_{u=1}^{m}x^u\right), \quad \textbf{[S40]}$$

where $\alpha$ is a parameter called the Lagrange multiplier.

To find the entropy-maximizing distribution satisfying the constraint $g_1=0$, we need to solve

$$\nabla L_1(x^1..x^m,\alpha)=0. \quad \textbf{[S41]}$$

Note that the partial differentiation of $L_1$ with respect to the Lagrange multiplier $\alpha$ is exactly equal to the first constraint function $g_1$, that is,

$$\frac{\partial L_1}{\partial\alpha}=g_1(x^1..x^m)=0.$$

By differentiating $L_1$ with respect to the components $x^u$ and setting the resulting equations equal to zero, we have

$$\frac{\partial L_1}{\partial x^u}=-1-\ln(x^u)-\alpha=0, \qquad u=1\ldots m. \quad \textbf{[S42]}$$

which yields the distribution

$$x^u=e^{-1-\alpha}, \qquad u=1\ldots m. \quad \textbf{[S43]}$$

By substituting this distribution in Eq. **S39** we find

$$x^u=\frac{1}{m}, \qquad u=1\ldots m. \quad \textbf{[S44]}$$

Thus, maximization of the entropy $H$ subject to the normalization constraint $g_1$ yields an equiprobable distribution.

The second constraint $g_2$ results from the condition on the cytoskeletal dynamics and writes as

$$g_2(x^1..x^m)=c-\sum_{u=1}^{m}\frac{x^u d^u}{\rho}, \quad \textbf{[S45]}$$

where $d^u$ is the shortest distance between the nucleus and edge $u$ and $c$ is a constant of order 1.

To account for both constraints $g_1$ and $g_2$, we introduce a second Lagrange multiplier $\beta$.

$$L_2(x^1..x^m,\alpha,\beta)=-\sum_{u=1}^{m}x^u\ln(x^u)+\alpha\left(1-\sum_{u=1}^{m}x^u\right)+\beta\left(c-\sum_{u=1}^{m}\frac{x^u d^u}{\rho}\right). \quad \textbf{[S46]}$$

Again, the maximum of the function $L_2(x^1..x^m,\alpha,\beta)$ is found by taking derivatives with respect to the components $x^u$ and setting the resulting equations equal to zero.

$$\frac{\partial L_2}{\partial x^u}=-1-\ln(x^u)-\alpha-\beta\frac{d^u}{\rho}=0, \qquad u=1\ldots m. \quad \textbf{[S47]}$$

This calculation yields a typical distribution $x^u$ scaling exponentially with the microtubule length $d^u$:

$$x^u=e^{-1-\alpha-\beta d^u/\rho}, \qquad u=1\ldots m. \quad \textbf{[S48]}$$

Here again, the values of $\alpha$ and $\beta$ must satisfy the two constraint equations. By analogy with statistical thermodynamics, we introduce the partition function $Z^{-1}=e^{-1-\alpha}$. Then, the values of $Z$ and $\beta$ must satisfy the system of equations

$$Z=\sum_{u=1}^{m}e^{-\beta d^u/\rho} \qquad c\rho Z=\sum_{u=1}^{m}d^u e^{-\beta d^u/\rho}. \quad \textbf{[S49]}$$

Although $\beta$ could in principle be expressed explicitly in terms of the microtubule length $d^u$, the presence of the unknown parameter $c$ makes that step irrelevant. We have thus measured $\beta$ experimentally. Future experiments performed on cells with fixed geometry will allow us to test how $\beta$ is set at the molecular level.

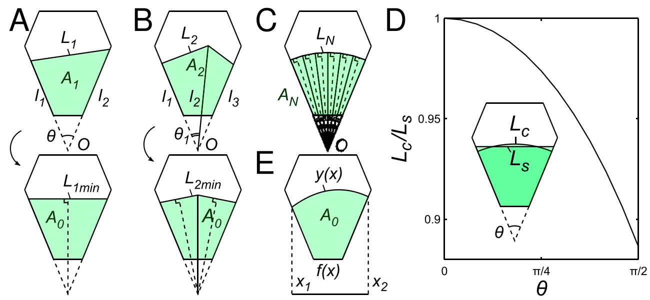


**Fig. S1.** Geometrical properties of the division plane. (*A*) Division of a polygonal cell by a straight line. (*B*) Division of a polygonal cell by two connected line segments. (*C*) Division of a polygonal cell by *N* connected line segments. (*D*) Length ratio between the curved and straight walls as a function of the angle $\theta$. (*E*) Division of a polygonal cell of equation $f(x)$ by a curve of equation $y(x)$ meeting the edges at points $(x_1, f(x_1))$ and $(x_2, f(x_2))$.

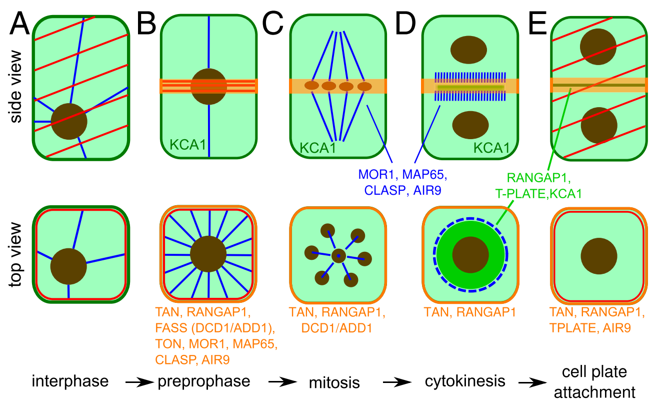


**Fig. S2.** Overview of the molecular detail for plant cell division. (*A*) Interphase. (*B*) Preprophase. (*C*) Mitosis. (*D*) During early cytokinesis, the new cell plate expands outward from the cell center. (*E*) At the end of cytokinesis, the cell plate meets the mother cell at the location of the preprophase band. Red: cortical microtubules. Blue: intracellular cytoskeleton.

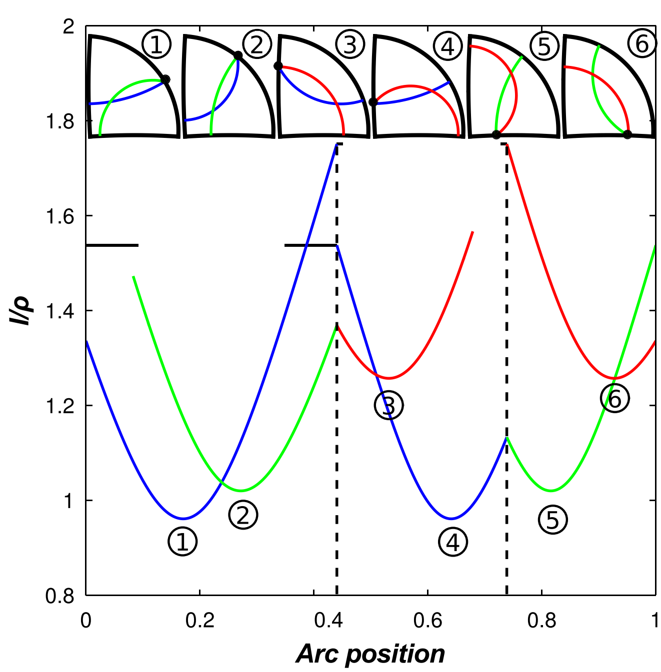


**Fig. S3.** Configuration space for dividing cells. For each arc position around the cell perimeter (the entire perimeter is normalized to 1), we compute numerically the shortest curves ending at this position and dividing the cell in two regions of equal size (see also Movie S3). The potential division planes of the cell correspond to the arc positions yielding the curves of minimal length for the edge pair under consideration. All possible edge pairs or division types are labeled with their own color.

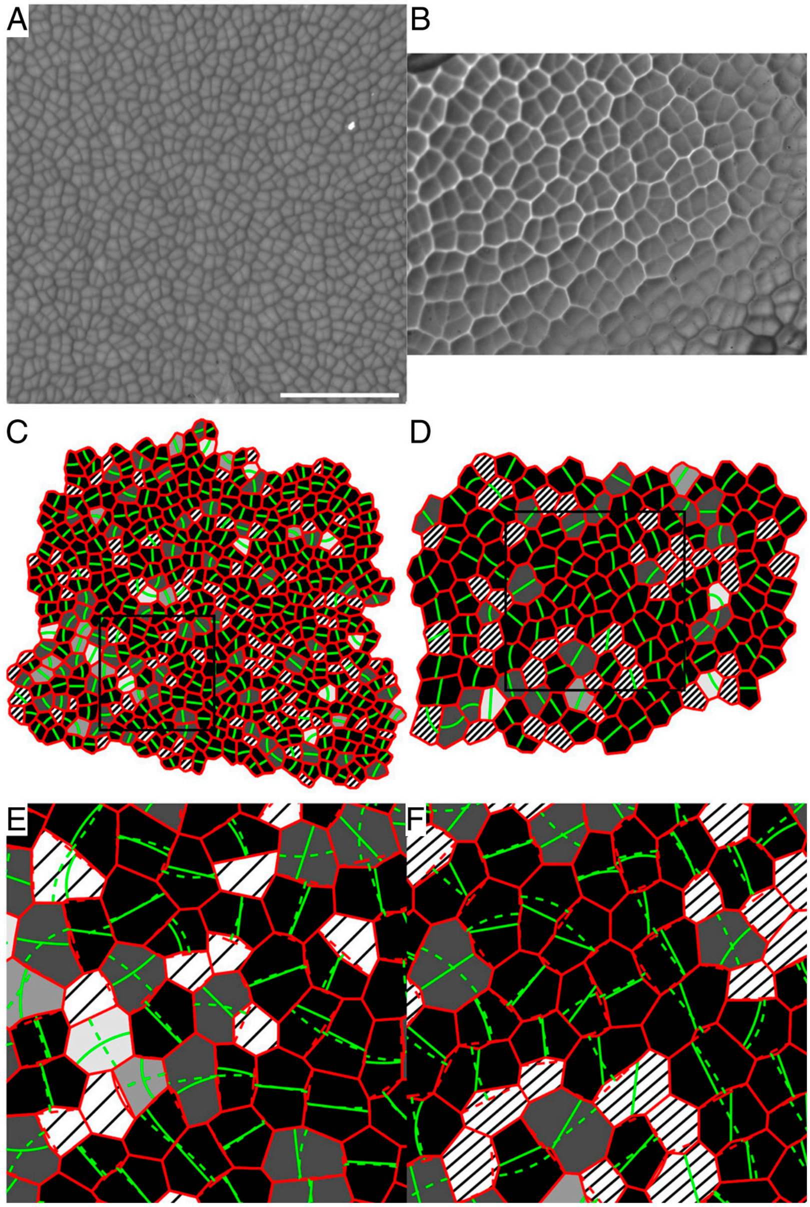


**Fig. S4.** Division of polygonal cells. (*A*) Scanning electron micrograph of the shoot apical meristem of the angiosperm *Zinnia elegans*. (*B*) Epoxy imprint of the adaxial face of the frond of the fern *Microsorum punctatum*. (*C* and *D*) Extracted cellular pattern with cells colored according to the mode of division: from the shortest planes (black) to the fourth shortest (lightest shade of gray). Cross-hatching denotes cells that did not divide or, in a few cases, divided along a plane that is not one of the minimal area configurations. (*E* and *F*) Closeup of the cellular patterns. The solid lines and dashed green lines represent the observed and predicted division planes, respectively. The match in most cells is surprisingly accurate given that the predicted position and shape of the division plane is done without any fitting parameters. When the predicted and observed division planes depart from each other, we commonly observe that Sachs's rule is at fault; i.e., the daughter cells are not of equal size. In many cases, correcting for this bias in the size of the daughter cells would bring the observed and predicted division planes in register.

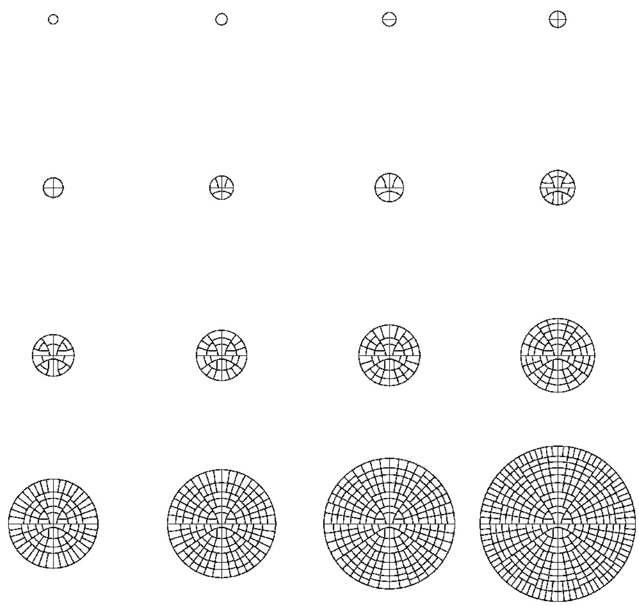

**Movie S1.** Simulation of the growth of the *Coleochaete* thallus. The development is modeled as a dynamical system using a marginal growth field and Errera's rule of cell division; i.e., the cells are divided along the plane of least area that creates two daughter cells of equal size.
Movie S1 (AVI)

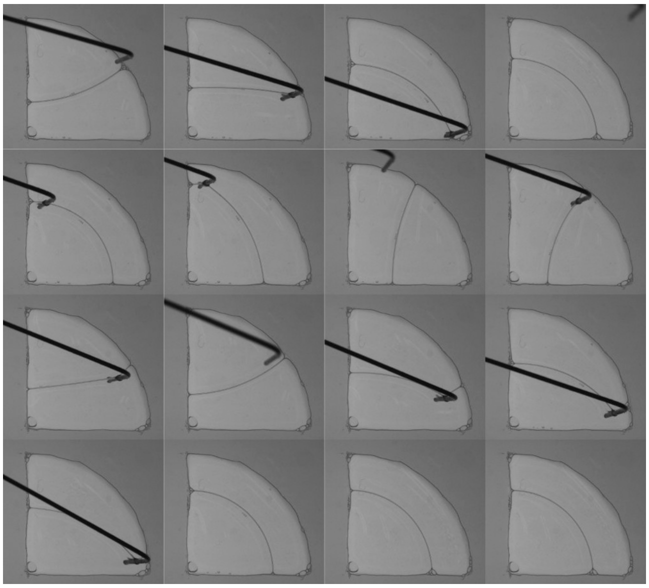

**Movie S2.** Alternative equilibrium configurations for two soap bubbles confined to a quadrant. The displacement of the soap film separating the two bubbles reveals three equilibrium configurations.
Movie S2 (AVI)

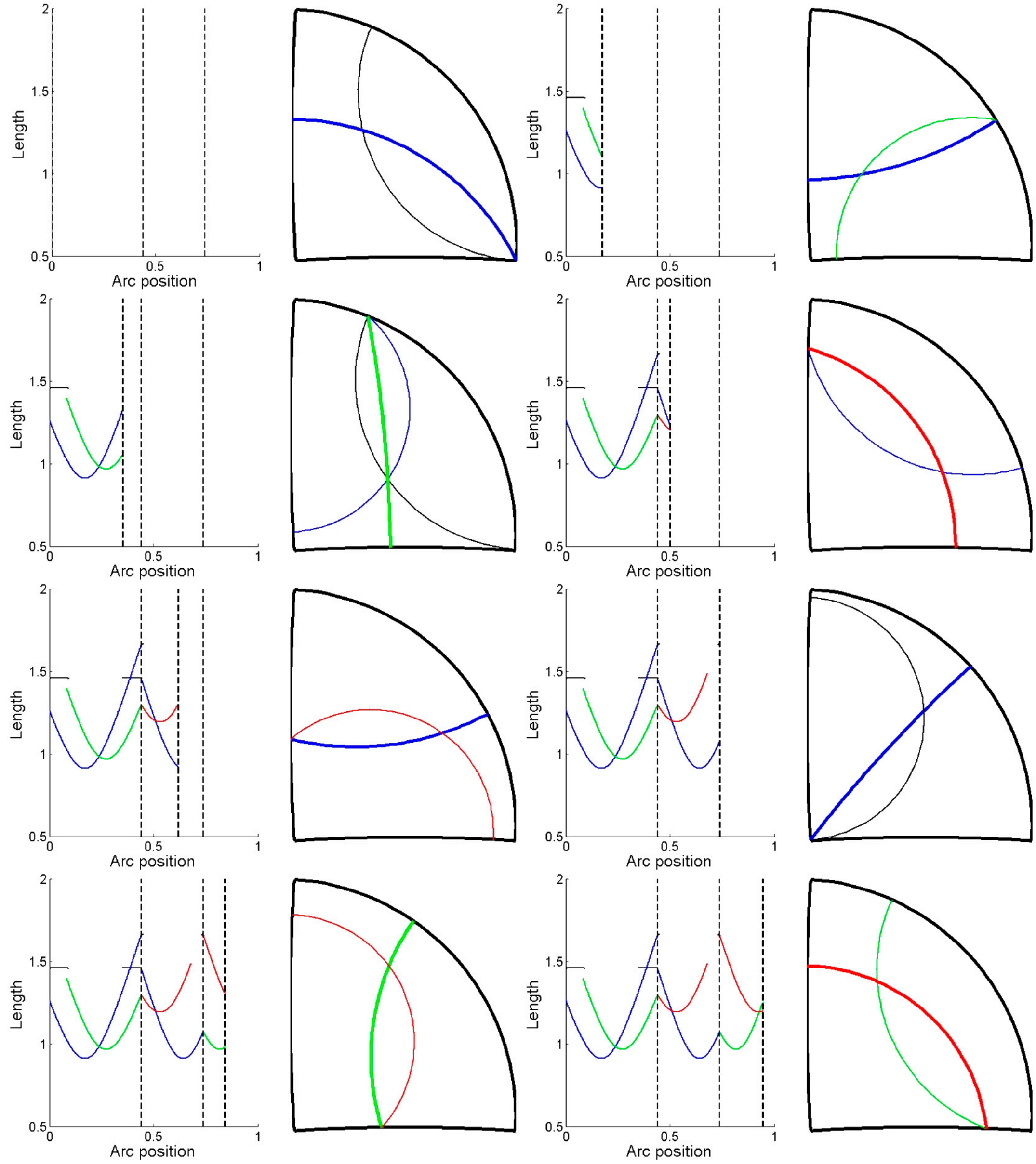


**Movie S3.** Numerical exploration of the configuration space. For each arc position around the cell perimeter (the entire perimeter is normalized to 1), we compute numerically the shortest curves ending at this position and dividing the cell in two regions of equal size. The potential division planes of the cell correspond to the arc positions yielding the curves of minimal length for the edge pair under consideration. All possible edge pairs or division types are labeled with their own color.

Movie S3 (AVI)